Weissenberg Reflection High-Energy Electron Diffraction for Surface Crystallography

Tadashi Abukawa,* Tomoyuki Yamazaki, Kentaro Yajima, and Koji Yoshimura

Institute of Multidisciplinary Research for Advanced Material, Tohoku University, Sendai 980-8577, Japan

(Received 16 August 2006; published 13 December 2006)

The principle of a Weissenberg camera is applied to surface crystallographic analysis by reflection high-energy electron diffraction. By removing inelastic electrons and measuring hundreds of patterns as a function of sample rotation angle ϕ, kinematical analysis can be performed over a large volume of reciprocal space. The data set is equivalent to a three-dimensional stack of Weissenberg photographs. The method is applied to analysis of an Si(111)-$\sqrt{3} \times \sqrt{3}$-Ag surface, and the structural data obtained are in excellent agreement with the known atomic structure.

DOI: 10.1103/PhysRevLett.97.245502 PACS numbers: 61.14.Hg

Electron diffraction techniques such as low-energy and reflective high-energy electron diffractometry (LEED, RHEED) have played an important role in surface crystallographic studies [1–3]. However, as dynamical effects are inherent in electron diffraction, simple kinematical theory cannot be strictly applied for structural analyses. Although dynamical analysis has recently become practical [2,3], LEED and RHEED retain the inherent disadvantage of being dynamical processes, in contrast to more reliable kinematical diffraction methods such as surface x-ray diffraction (SXRD) [4].

Several attempts have been made to realize a direct structure determination by a kinematical-based model for electron diffraction. Correlated thermal diffuse scattering [5] reconstructs the surface atomic arrangement based on electron diffuse scattering, while the constant momentum averaging (CMTA) method for LEED aims to suppress dynamical effects by data averaging. CMTA was originally proposed by Lagally *et al.* in 1973 [6], and has recently been revived with the assistance of new technologies [7–9]. These two examples both employ four primary approaches to realizing kinematical analysis of electron diffraction: large data volumes, data averaging in reciprocal space, multiple incident angles (and/or energies), and elimination of inelastically scattered electrons. The first three techniques attempt to dilute the dynamical effects by averaging a large number of data, while the elimination of inelastic electrons reduces the chance of dynamical effects occurring by guaranteeing a short penetration path due to the inelastic mean free path of the electrons.

When these techniques are applied to RHEED analysis, the advantages of RHEED become apparent. The most attractive feature is the accessibility to a large volume of the reciprocal space, as demonstrated by Braun *et al.* [10] during substrate rotation. Most of the upper half of the reciprocal space can be accessed by azimuth rotation of the sample, the principle of which is identical to that of a Weissenberg camera for x-ray crystallography [11]. The method was first applied to obtain large three-dimensional (3D) images of the reciprocal space by Abukawa *et al.* [12] for an Si(111)-$\sqrt{3} \times \sqrt{3}$-Ag surface. The structural phase transition was discussed in that study on the basis of a qualitative analysis of Patterson function. Very recently, this approach has also been applied by Romanyuk *et al.* [13] to investigate the structure of $FeSi_2$/Si(111). Although several assumptions were required in order to solve the structure, the potential utility of the method was proved. It should be noted, however, that intrinsic structural complexity and the involvement of inelastic electrons may reduce the performance of the Patterson analysis.

In the present study, direct structural determination by a Weissenberg RHEED (W-RHEED) method with an energy filter is demonstrated for the first time. The principle of the method is identical to that of the Weissenberg camera for XRD [11], and the images obtained are treated as Weissenberg photographs.

The fundamental concept of the Weissenberg camera is shown in Fig. 1(a). The crystal is mounted in the camera with one of the crystal axes parallel to the rotation axis (ϕ). When the c axis of the crystal is set parallel in this manner, the slit acts as a window permitting only reflections with constant l index. As the crystal is rotated about the ϕ axis, various reflections of constant l are excited and captured via the slit. The film is linearly translated parallel to the ϕ axis synchronously with the rotation such that hk reflec-

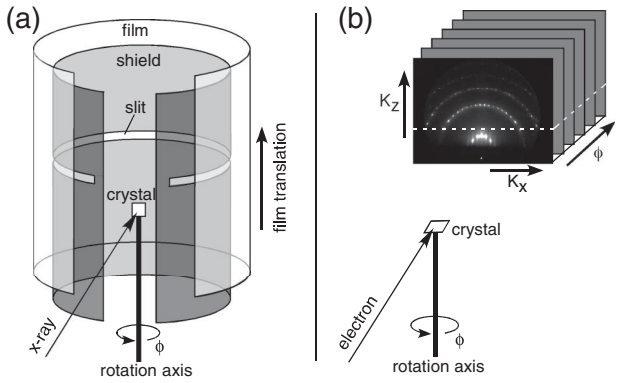

FIG. 1. (a) Schematic of x-ray Weissenberg camera. (b) Conceptual illustration of Weissenberg RHEED.

tions at constant l are unequivocally mapped on a two-dimensional (2D) map.

The concept of W-RHEED is illustrated schematically in Fig. 1(b). In addition to a conventional RHEED system, a precise ϕ rotation function is required, as well as a high-pass energy filter before the screen (not shown). The crystal is mounted with surface normal parallel to the ϕ rotation axis. Instead of using a slit and film translation, hundreds of screen images are captured by a charge-coupled device (CCD) camera and stored on a computer as a function of the rotation angle ϕ. Using a virtual spherical screen, the diffraction images are stored in coordinates of the electron wave vector (K_X, K_Z), where the X axis is perpendicular to both the surface normal and the incident beam, and the Z axis is parallel to the surface normal. A 3D data set $I(K_X, K_Z, \phi)$ is then assembled as shown in Fig. 1(b), referred to hereafter as ϕ-scan data. Typical horizontal slices of ϕ-scan data obtained in experiments are shown in Fig. 2. The horizontal slices are equivalent to the Weissenberg photograph of XRD [11]. The primary advantage of the present method is the ability to acquire a 3D stack of Weissenberg photographs from a single ϕ-scan data set. Indexing and digitizing the spot intensity on each Weissenberg photograph gives diffraction data in the 3D reciprocal space $I(\mathbf{s})$, as shown in Fig. 2(c).

As a further step, several ϕ-scan data sets measured with different incident glancing angles and/or energies can be averaged, although the speed of analysis will be substantially reduced. The method is evaluated in the present study without multiscan averaging.

The W-RHEED method is evaluated here in application to the structural analysis of an Si(111)-$\sqrt{3} \times \sqrt{3}$-Ag surface. The inequivalent triangle (IET) structure is now accepted to be the ground structure of this surface below ~130 K [14,15]. As the Patterson map for this surface has already been reported [15], this surface is ideal for evaluation of the proposed method. Although the structural phase transition from the IET ground state to another room-temperature phase has been reported for this surface [12,15–18], the experiments conducted in the present study focus on analysis of the ground state.

Experiments were performed using an ultrahigh vacuum (UHV) W-RHEED system consisting of an electron gun, an energy filter, a phosphor screen, a five-axis sample manipulator, and a K cell for Ag deposition. The high-pass energy filter consisted of three spherical retarding grids, constructed in accordance with Ref. [19], and had an energy resolution of $\lesssim 4$ eV at 10 keV. The primary beam energy for RHEED measurements was 10 keV. The energy-filtered RHEED pattern displayed on the phosphor screen was captured by a CCD video camera. The θ and ϕ rotations of the sample manipulator were motorized.

A mirror-polished Si(111) wafer (0.004 Ω cm, As doped) with dimensions of $25 \times 3 \times 0.6$ mm^3 was used as a substrate. The sample was resistively heated and then

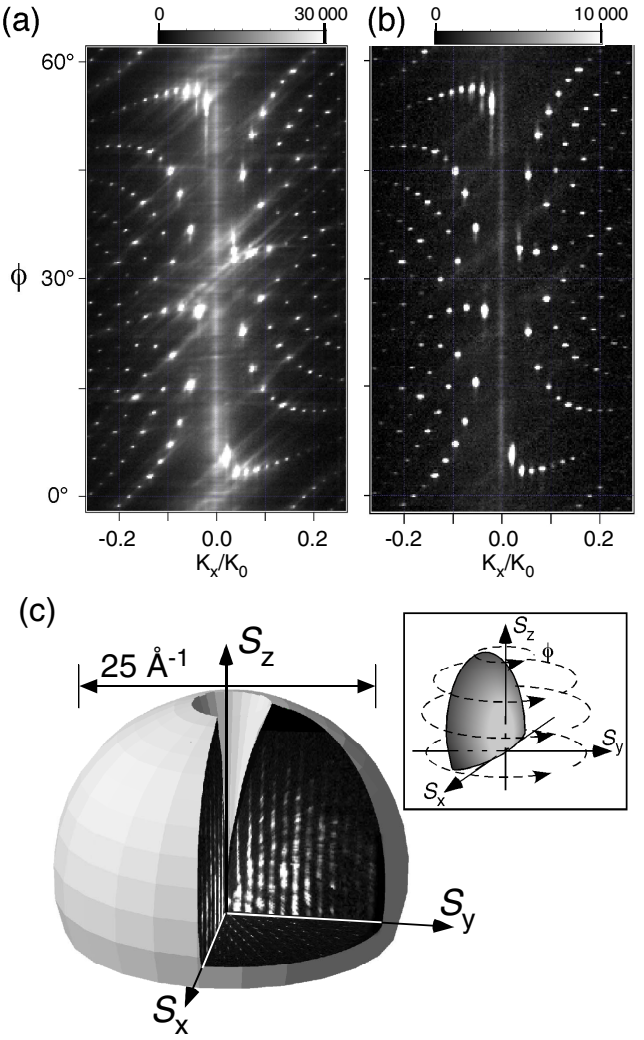

FIG. 2 (color online). (a) Weissenberg map (horizontal section at $K_z = 2.2$ Å^{-1}) for an Si(111)-$\sqrt{3} \times \sqrt{3}$-Ag surface at 105 K. (b) Same map after elimination of inelastic electrons by the energy filter. (c) Observable volume in the reciprocal space by the W-RHEED method, where a quadrant has been cut to show internal sections, and $\mathbf{s} = (s_x, s_y, s_z)$ is the scattering vector. (Inset) Rotation of the Ewalt sphere about the ϕ axis.

cooled via Cu braids connected to a liquid-N_2 reservoir. The sample temperature (below room temperature) was measured by a thermocouple attached to an Mo sample holder. The ultimate temperature was 105 K, at which ϕ rotation was still possible. A clean Si(111)-7×7 surface was prepared by flashing for 5 s at 1500 K followed by annealing for 5 min at 1250 K under UHV. A well-ordered Si(111)-$\sqrt{3} \times \sqrt{3}$-Ag surface was obtained by following the procedure in Ref. [20]. Very sharp $\sqrt{3} \times \sqrt{3}$ RHEED patterns were obtained for this sample. The RHEED results also reveal an abrupt intensity change at 130 K, indicative of a phase transition [12,15,16].

W-RHEED analysis of the Si(111)-$\sqrt{3} \times \sqrt{3}$-Ag surface at 105 K was conducted rotating the surface by 60° from

the $[2\bar{1}\,\bar{1}]$ incidence to $[1\bar{2}1]$ incidence, taking advantage of the C_{3V} symmetry. The measurement interval was 0.1°, which is considered sufficiently fine for a continuous survey of the reciprocal space. Thus, a total of $\gtrsim 600$ RHEED patterns were obtained in a single ϕ-scan measurement run. Although several ϕ-scan measurements were performed at different glancing angles, only the result for a glancing angle of 2.85° is reported here. A typical scan took $\lesssim 90$ min. The present W-RHEED technique is therefore a very fast method for scanning a large volume of the reciprocal space.

Horizontal slices of the ϕ-scan data are shown in Fig. 2 for the Si(111)-$\sqrt{3}\times\sqrt{3}$-Ag surface at 105 K with a glancing angle of 2.85°. With the threshold energy of the energy filter set at 220 V below the elastic peak, Kikuchi lines are clearly apparent [Fig. 2(a)] as oblique parallel lines, whereas the lines are very faint with the threshold energy set at 5.5 V below the elastic peak [Fig. 2(b)]. This is consistent with previous results for energy-filtered RHEED [19]. The Kikuchi lines usually disturb RHEED spot measurements. These results therefore demonstrate the suppression of one of dynamical effects by the elimination of inelastic electrons.

The Patterson function $P(\mathbf{r})$ was obtained by Fourier transformation of $I(\mathbf{s})$ obtained using a threshold energy of 5.5 eV. Only the positive real part was selected as the meaningful Patterson function from the complex function obtained by fast Fourier transformation (FFT). Relative positions between atoms in the structure are mapped in $P(\mathbf{r})$, that is, a spot appears in $P(\mathbf{r})$ when $\mathbf{r}$ matches one of the interatomic vectors of the crystal. A horizontal slice of the $P(\mathbf{r})$ volume at $z = 0.0$ Å is shown in Fig. 3(a). The

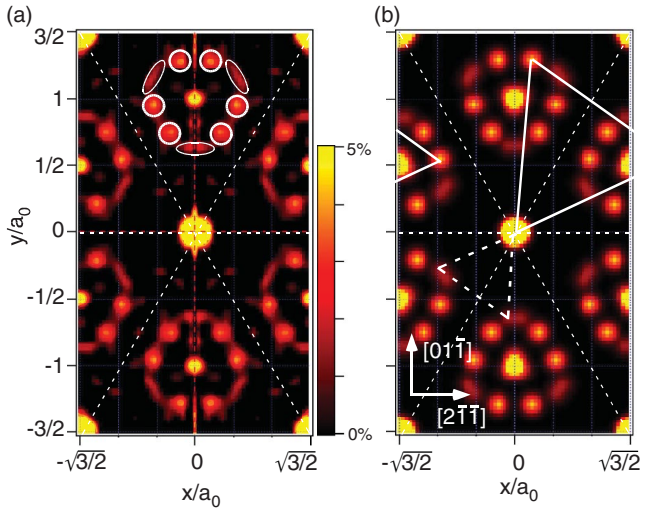

FIG. 3 (color). Horizontal sections of $P(\mathbf{r})$ at $z = 0.0$ Å. (a) Experimental results obtained by W-RHEED. Intensity is normalized by the maximum of $P(\mathbf{r})$ and from 0 to 5% is linearly mapped with the color scale. (b) Simulated results by the IET model for an Si(111)-$\sqrt{3}\times\sqrt{3}$-Ag surface. a_0 (= 3.84 Å) is the unit length of the Si(111)-1 × 1 lattice.

relative atomic positions within the same layer should be mapped in such a slice. The rectangular surface cell, which includes two $\sqrt{3}\times\sqrt{3}$ unit cells, produces 6 intense spots at a distance of $a_0 = 3.84$ Å from the origin. These spots mainly originate from the 1×1 triangular lattice of the substrate. The next most significant structures are the 6 satellite spots around each 1×1 spot, as marked in Fig. 3(a). Faint adjacent structures are also highlighted.

The same horizontal slice of $P(\mathbf{r})$ simulated using the IET model [14] is shown in Fig. 3(b). The dominant experimental structures are perfectly reproduced by the simulation. The IET structure is characterized by a rotated Ag triangle and Si triangle, as indicated in the figure by solid and broken lines, respectively. It is clear that the 6 satellite spots correspond to the interatomic vectors between Ag atoms of the IET structure, while the faint structures originate from the interatomic vectors between Si trimer atoms. The validity of the present Patterson function is confirmed by the coincidence with the Patterson function obtained by SXRD [15].

To demonstrate the capability of W-RHEED for 3D structural analysis, the $P(\mathbf{r})$ function was solved using the minimum function method, which is a fundamental x-ray crystallography method solving the Patterson function [11]. In general, the first step in solving $P(\mathbf{r})$ is to find a small cluster that repeatedly appears in $P(\mathbf{r})$. Such a repeated cluster may be the replicated footprint of an atomic cluster present in the surface structure. The minimum function is a special method for estimating the correlation between the cluster and $P(\mathbf{r})$. When the cluster consists of n atoms with positions expressed by $\mathbf{r}_i$, the minimum function $M(\mathbf{r})$ is defined as

$$M(\mathbf{r}) = \min\{P(\mathbf{r}-\mathbf{r}_1), P(\mathbf{r}-\mathbf{r}_2), P(\mathbf{r}-\mathbf{r}_n)\}, \quad (1)$$

where the function min{} gives a minimum value from the functions listed in the braces. If a suitable cluster is chosen, the atomic positions viewed from the cluster, which is the information desired, should appear directly in $M(\mathbf{r})$.

The Ag trimer outlined by solid lines in Fig. 3(b) is selected as the cluster for the minimum function. This is a fundamental building block of one of the two equivalent domains of the IET structure, where each domain consists of the Ag trimer rotating clockwise or counter clockwise. The side length and rotation angle of the trimer, which can be measured from Fig. 3(a), are 4.95 Å and 5° clockwise. Thus, the vectors of the trimer atoms are given by $\mathbf{r}_1 = (0.0, 0.0, 0.0)$, $\mathbf{r}_2 = (0.43, 4.93, 0.0)$, and $\mathbf{r}_3 = (4.49, 2.09, 0.0)$. Important horizontal sections of the $M(\mathbf{r})$ thus obtained are shown in Figs. 4(a)–4(c) using a common color scale. A top view of the corresponding IET model (clockwise domain) is also shown in Fig. 4(d). Figure 4(a) shows the section at $z = 0.0$ Å, corresponding to the Ag trimer plane. As shown with broken circles and lines in the figure, the observed spots perfectly reproduce the Ag trimers of the IET structure. The Si trimers of the

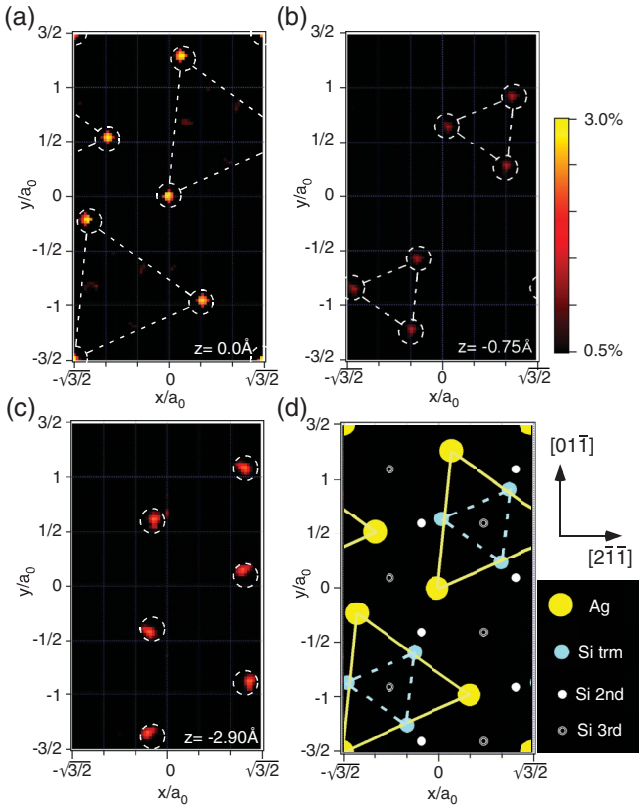

FIG. 4 (color). (a)–(c) Horizontal sections of $M(\mathbf{r})$ at $z = 0.0$ (a), -0.75 (b) and -2.9 Å (c). Intensity is normalized by the maximum of $P(\mathbf{r})$ and from 0.5 to 3% is linearly mapped with the color scale. (d) Projected top-view of the IET (clockwise) model for the Si(111)-$\sqrt{3} \times \sqrt{3}$-Ag surface.

IET structure appear 0.75 Å below the Ag trimer [Fig. 4(b)], located laterally in the correct position with reference to the Ag trimer in Fig. 4(a). The side of the trimer and the rotation angle were determined from the present results to be 2.45 Å and 5°. The second layer Si, that is, the upper atoms of the first Si double layer, appear 2.90 Å below the Ag trimer. The substrate structure could be observed down to 10 Å below the surface in $M(\mathbf{r})$ (data not shown). The spot size in the z direction was nearly equal to that in the lateral direction.

The IET structure was thus successively reproduced by the $M(\mathbf{r})$ function obtained from the W-RHEED measurements. For kinematical analysis, large amounts of data are required, and inelastic electrons must be filtered out of the diffracted beams. The proposed method achieves both requirements, and has the advantage of providing fast measurement of a large reciprocal volume.

Weissenberg RHEED was introduced as a method for kinematical study of surface structures. The method involves acquisition of hundreds of RHEED patterns as a function of azimuthal angle ϕ, and represents a fast method for acquiring diffraction data over a wide range of reciprocal space. The 3D Patterson function obtained for an Si(111)-$\sqrt{3} \times \sqrt{3}$-Ag surface by this method was shown to be closely consistent with the known atomic structure of the surface. It was also demonstrated that the structure can be directly solved from the Patterson function by a standard method in x-ray crystallography.

This work was supported in part by Grants-in-Aid for Scientific Research (A) No. 12354003, the Encouragement of Young Scientist (A) No. 14702007, and Scientific Research (B) No. 17360016 from the Ministry of Education, Culture, Sports, Science and Technology of Japan. The authors are grateful to Professor S. Kono for continuing support.

*Electronic address: abukawa@tagen.tohoku.ac.jp

[1] J. B. Pendry, *Low Energy Electron Diffraction* (Academic, London, 1974).
[2] A. Ichimiya and P. Cohen, *Reflevtion High-energy Electron Diffraction* (Cambridge University Press., Cambridge, England, 2004).
[3] M. A. Van Hove, W. H. Weinberg, and C.-M. Chan, *Low-Energy Electron Diffraction: Experiment, Theory and Surface Structure Determination*, (Springer-Verlag, Berlin, 1986).
[4] I. K. Robinson and D. J. Tweet, Rep. Prog. Phys. **55**, 599 (1992), and references therein.
[5] T. Abukawa and S. Kono, Prog. Surf. Sci. **72**, 19 (2003).
[6] M. G. Lagally, T. C. Ngoc, and M. B. Webb, Phys. Rev. Lett. **26**, 1557 (1971).
[7] H. Wu and S. Y. Tong, Phys. Rev. Lett. **87**, 036101 (2001).
[8] Celia Rogero, Jose-Angel Martin-Gago, and P. L. d. Andres, Phys. Rev. B**67**, 073402 (2003).
[9] J. Wang, H. Wu, Ricky So, Y. Liu, M. H. Xie, and S. Y.Tong, Phys. Rev. B **72**, 245324 (2005).
[10] W. Braun, H. Moller, and Y.-H. Zhang, J. Vac. Sci. Technol. B **16**, 1507 (1998).
[11] For example, M. F. C. Ladd and R. A. Palmer, *Structure Determination by X-ray Crystallography* (Plenum, New York, 1993), 3rd ed.
[12] T. Abukawa, T. Yamazaki, K. Yajima, and S. Kono, *22nd European Conference on Surface Science, Prague, Czech Republic, September 2003*, Abstract 16 906.
[13] O. Romanyuk, K. Kataoka, F. Matsui, K. Hattori, and H. Daimon, Czech. J. Phys. **56**, 267 (2006).
[14] H. Aizawa, M. Tsukada, N. Sato, and S. Hasegawa, Surf. Sci. **429**, L509 (1999).
[15] H. Tajiri, K. Sumitani, and S. Nakatani *et al.*, Phys. Rev. B **68**, 035330 (2003).
[16] H. Nakahara, T. Suzuki, and A. Ichimiya, Appl. Surf. Sci. **234**, 292 (2004).
[17] Y. Fukaya, A. Kawasuso, and A. Ichimiyal, J. Surf. Sci. Nanotechnology **3**, 228 (2005).
[18] K. Sakamoto, T. Suzuki, and K. Mawatari *et al.*, Phys. Rev. B **73**, 193303 (2006).
[19] Y. Horio, Jpn. J. Appl. Phys. **35**, 3559 (1996).
[20] R. I. G. Uhrberg, H. M. Zhang, T. Balasubramanian, E. Landemark, and H. W. Yeom, Phys. Rev. B **65**, 081305(R) (2002).